JOURNAL OF MATERIALS SCIENCE 35 (2000) 5215–5223

Phase structures, transition behavior and surface alignment in polymers containing rigid-rod backbones with flexible side chains

Part VI *Novel band structures in a combined main-chain/side-chain liquid crystalline polyester: From liquid crystal to crystalline states*

J. J. GE, J. Z. ZHANG, WENSHENG ZHOU, C. Y. LI, SHI JIN, B. H. CALHOUN, SHY-YEU WANG, F. W. HARRIS, S. Z. D. CHENG*
The Maurice Morton Institute and Department of Polymer Science, The University of Akron, Akron, Ohio 44325-3909, USA
E-mail: cheng@polymer.uakran.edu

Physical origins of banded structures appearing on different length scales have been investigated using polarized light and atomic force microscopies (PLM and AFM), polarized Fourier Transform infrared spectroscopy (FT-IR) and wide angle X-ray diffraction (WAXD) in a combined main-chain/side-chain liquid crystalline (LC) polyester, PEFBP(*n*). This series of PEFBP(*n*) polymers was synthesized from the polycondensation of 2,2′-bis(trifluoromethyl)-4,4′-biphenyldicarbonyl chloride with 2,2′-bis{ω-[4-(4-cyanophenyl)-phenyoxy]-*n*-alkoxycarbonyl]}-4,4′-biphenyl diol. In this paper, we focus on one polymer [PEFBP($n = 11$)] of this series to illustrate the band structural formation on different length scales during the evolution from liquid crystal to crystalline states. Alternating bands of the films mechanically-sheared at 190 °C are formed with a spacing of 3 ± 0.5 μm in PLM, and recognized to be primary bands. PLM and AFM results show that these bands are seen due to the change of optical birefringence constructed mainly by alternating film thickness (and thus, retardation). Based on polarized FT-IR results, both the backbones and side chains of the polymers are orientated parallel to the shear direction. Secondary fibrillar bands develop within the primary bands after the sample is subsequently crystallized at 105 °C. These bands show a zigzag arrangement and possess a lateral size of 250 ± 50 nm determined by AFM. High resolution AFM observations illustrate that these bands consist of aggregated edge-on crystal lamellae having a thickness of approximately 20 nm. The lamellar crystals are assembled together and lie across the film thickness direction. The mechanism for the formation of these secondary zigzag bands originates from the expansion of the lattice dimension along the chain direction on a molecular scale during the nematic to crystalline phase transition and crystallization in the partially confined LC primary bands, which form macroscopic zigzag buckling.

1. Introduction

Recently, one-dimensional periodic band structures were characterized in lyotropic liquid crystalline (LC) polymers, such as oriented secretions of natural silk glands (*Bombyx mori*) or spider ampullae (*Nephila clavipes*) [1], synthetic Kelvar fibers, poly(g-benzyl L-glutamate) (PBLG), hydroxypropyl cellulose (HPC) [2–5], and thermotropic LC polymers, in response to a variety of external flow influences like uniaxial fiber spinning, mechanical shear deformation and even crystallization [6–10]. The origin of the band structures induced by crystallization is, however, not well understood [10, 11]. Further investigation of the underlying physical mechanisms of crystallization-induced band structures in polymers, which must be associated with supra-molecular organization, as implied by the band structures on different length scales, is of interest.

The band structure is traditionally an important characteristic feature in oriented lyotropic and thermotropic LC polymers. Commonly, the bands are

* Author to whom all correspondence should be addressed.

periodic straight lines or zones of light and dark, are observed macroscopically in PLM, and lie normal to the shear direction. Although the mechanism of the band formation is still far from a quantitative understanding, it is generally believed that the formation of bands with a periodical arrangement is related to a relaxation of oriented viscoelastic LC polymer fluids after the release of external force fields [11].

Due to one-dimensional arrays of shear-induced defects that could substantially affect physical properties, great efforts have been made to optimize these properties of flow-influenced LC polymers [12]. All these optimizations require a deep understanding of structure-property-processing relationships, under which band structures in different length scales play important roles. In the structural and morphological analyses, much progress has been achieved using different techniques such as polarized light microscopy (PLM) [1–3, 6–11], small angle light scattering [4, 5], transmission electron microscopy [8, 11–14], scanning electron microscopy [15, 16], and optical diffraction [6, 8, 17]. These techniques provide specific measured structural or morphological parameters which represent band defects in a two-dimensional (2-D) anisotropic array from macroscopic down to microscopic scales. In the past few years, scanning probe microscopies, such as atomic force microscopy (AFM), have been developed that show a promising elucidation of materials' surface topologies on a molecular level [18]. In particular, these new techniques allow us to visualize the presence of 3-D intrinsic topologies and defects in real space including band structures [19].

In our laboratory, a series of main-chain/side-chain LC polyesters was synthesized via a polycondensation of 2,2′-bis(trifluoromethyl)-4,4′-biphenyldicarbonyl chloride with 2,2′-bis{ω-[4-(4-cyanophenyl)-phenyoxy]-*n*-alkoxycarbonyl]}-4,4′-biphenyl diol [PEFBP(*n*), *n* being the number of methylene units] [20]. The structures, phase transitions, morphology, and even-odd effect on the phase transitions have been reported [21–23]. Pendant 4-cyanophenyl side chains are attached at the 2,2′-positions of biphenylene backbones through methylene units, leading to the formation of LC phases. The substituted biphenylenes in the aromatic backbones are forced to adopt a nearly 90° twisted chain conformation due to steric hindrance. These polymers with pendant side chains possess numerous potential applications in specific linear and nonlinear optical devices [24–26].

In this paper, the combined techniques of PLM, AFM and wide angle X-ray diffraction (WAXD) methods are used to investigate band structures of one main-chain/side-chain LC polyester PEFBP($n = 11$) on different length scales. In particular, after this polymer is mechanically sheared in the nematic (N) phase, we recognize the existences of not only the traditional band structures on the micrometer scale, but also sub-band structures formed after crystallization within the traditional bands. Formation mechanisms of these banded structures are discussed. A new concept, macroscopic self-elongation along the shear direction, can be proposed in oriented PEFBP($n = 11$), when a phase transition occurs from the N phase to the crystal (K) phase. This is attributed to a microscopic lattice expansion along the oriented chain direction after crystallization. The chain molecules are buckled and responsible for the zigzag arrangement within the transitional LC band structure.

2. Experimental section

2.1. Materials and samples

The synthetic strategy and physical characterization of this combined liquid crystal polyester has been reported elsewhere [20]. This investigation focuses on polyester containing eleven methylene units in the side chains, abbreviated as PEFBP($n = 11$) with the chemical structure shown below

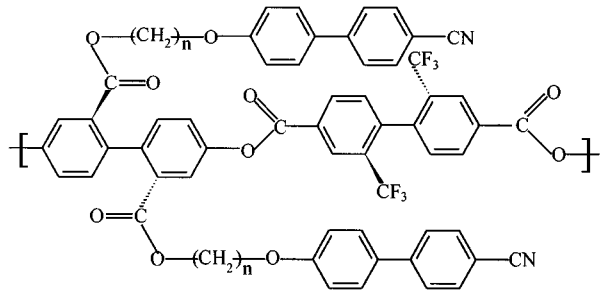

The intrinsic viscosity of this fractionated polymer using chloroform is 0.04 m^3/kg measured at 30 °C. The number average molecular weight of PEFBP($n = 11$) was 15,600 g/mol and the polydispersity after specific fractionation was 1.10, which was determined by gel permeation chromatography with tetrahydrofuran (THF) columns at 25 °C, and calibrated with standard polystyrene samples.

The films having a typical thickness of approximately 1–2 μm were sheared uniaxially by a mechanical force on the glass substrate at a rate of 10 mm/s at a temperature between the crystal melt (170 °C) and the isotropization temperature (193 °C). The shear process was carried out under a pressure of approximately 10^5 Pa and immediately quenched to room temperature after shearing. The films were then crystallized at 105 °C at different times and examined in PLM, polarized FT-IR, AFM and WAXD experiments.

2.2. Equipment and experiments

Morphological observations on a micrometer scale were conducted on an Olympus (HB-2) PLM coupled with a Mettler hot stage FP-90. For morphologies over a broad length scale from micrometers to nanometers, an atomic force microscope (AFM, Digital Instruments Nanoscope IIIa) was utilized in the tapping mode to study the detailed morphological changes on the surface and near surface of the sheared films.

WAXD two-dimensional experiments were conducted on a Rigaku 18 kW rotating-anode generator (Cu K_α) coupled with an image plate. The X-ray beams were monochromatized using well-defined graphite crystals. The reflection peak positions and

widths observed were calibrated with silicon crystals of known crystal sizes in the high angle region ($2\theta > 15^\circ$) and silver behenate in the low angle region ($2\theta < 15^\circ$). The film samples were folded at least three times along the shear direction to increase the sample thickness and shorten the experimental time. The WAXD patterns obtained from the oriented films were continuously computer-refined with the least square-root regressions. The air scattering spectrum is subtracted automatically from the reference spectrum.

Polarized FT-IR experiments of sheared films were conducted on a Mattson Galaxy Series FT-IR 5000 spectrometer equipped with a He : Neon laser source and a polarizer rotation stage in a transmission geometry. The accuracy of the wavenumber is limited within 4 cm^{-1}. A rotation stage was used to control the sample orientation with respect to the polarized IR beam. The rotating range was between 0° and 90° with an angular accuracy of $\pm 0.5^\circ$ in the azimuthal direction. The sample was uniaxially sheared at 190 °C on a KBr substrate using a mechanical force. The thermal histories were identical to the samples used in PLM and WAXD experiments.

3. Results and discussion

Fig. 1 exhibits a PLM observation of uniformly alternating band structures (recognized as *primary bands*) of PEFBP($n = 11$) films with a periodic spacing of 3 ± 0.5 μm nearly parallel to each other, induced by mechanical shearing at 190 °C. The normal direction of these bands is parallel to the shear direction (represented by an arrow in the figure). The band spacing is dependent on the shear conditions, such as temperature, shear rate, and pressure. The possible formation mechanism of this kind of LC bands has stimulated quite extensive discussions in the past two decades [7, 8, 13, 14]. It is commonly understood that the band formation is due to the orientation of the main-chain LC molecules under shear and a slight relaxation after the shear which generates differences in the birefringence. Chain molecules are oriented parallel to the shear direction, namely, it is parallel to the band normal. However, in the case of main-chain/side-chain LC polymers, backbone and side chain orientations after shear have not been studied. In hairy-rod polymers, it has been reported that the aliphatic side chains that consist of methylene units are packed perpendicular to the backbone chains to form a sanidic (board-like) structure [27–30].

Fig. 2 shows a set of polarized FT-IR spectra on a sheared PEFBP($n = 11$) film, which can directly distinguish the group orientations of both the backbones and side chains via changes of vibration intensities, and therefore, identify the overall orientations of these two components. The rotating stage is controlled between 0° to 90° with an interval of 5°. A characteristic vibration of the side chains is the CN groups in the 4-cyanobiphenyl mesogens at 2225 cm^{-1} (the stretching vibration). The intensity of this vibration clearly increases as the polarizer angle changes from 90° (perpendicular to the shear direction) to 0° (parallel to the shear direction). This indicates that the 4-cyanobiphenyl mesogens in the side chains are arranged almost parallel to the shear direction. Furthermore, in the wave-number region between 600 and 1000 cm^{-1}, vibration bands at 919, 855, 823, and 747 cm^{-1} represent the out-of-plane CH bending of the substituted phenylenes in both the backbones and side chains. Intensities of these bands all decrease when the polarizer angle changes from 90° to 0° with respect to the band normal. On the other hand, the intensity of phenylene in-plane CH bending at 1004 cm^{-1} is conversely increased. The minimum intensity of the carbonyl vibration at 1710 cm^{-1} indicates that the side-chain carbonyl stretching is 15° off the shear direction (as indicated by the * in Fig. 2). The main-chain carbonyl stretching vibration at 1745 cm^{-1} is more intense in

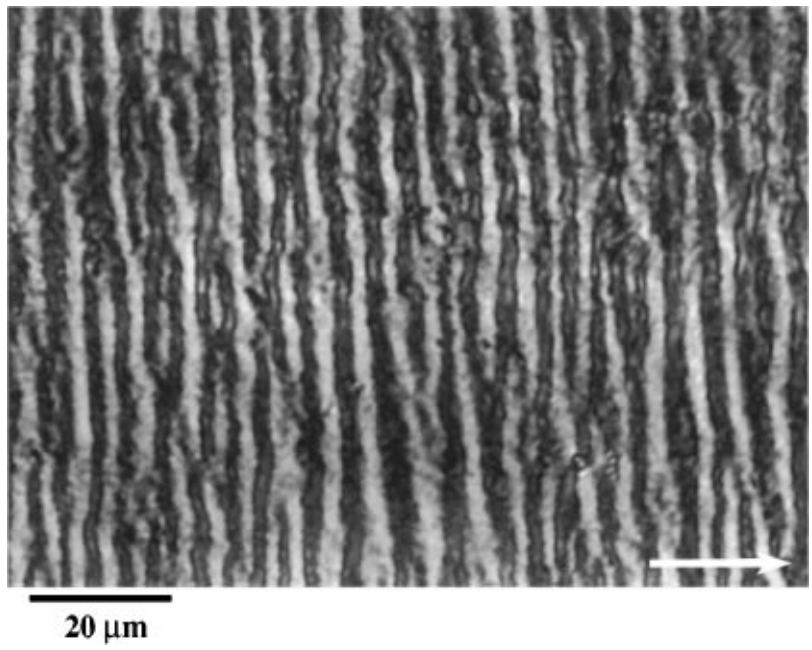

Figure 1 PLM micrograph of directly sheared specimens for PEFBP($n = 11$) after rapid quenching to below T_g (recorded at room temperature).

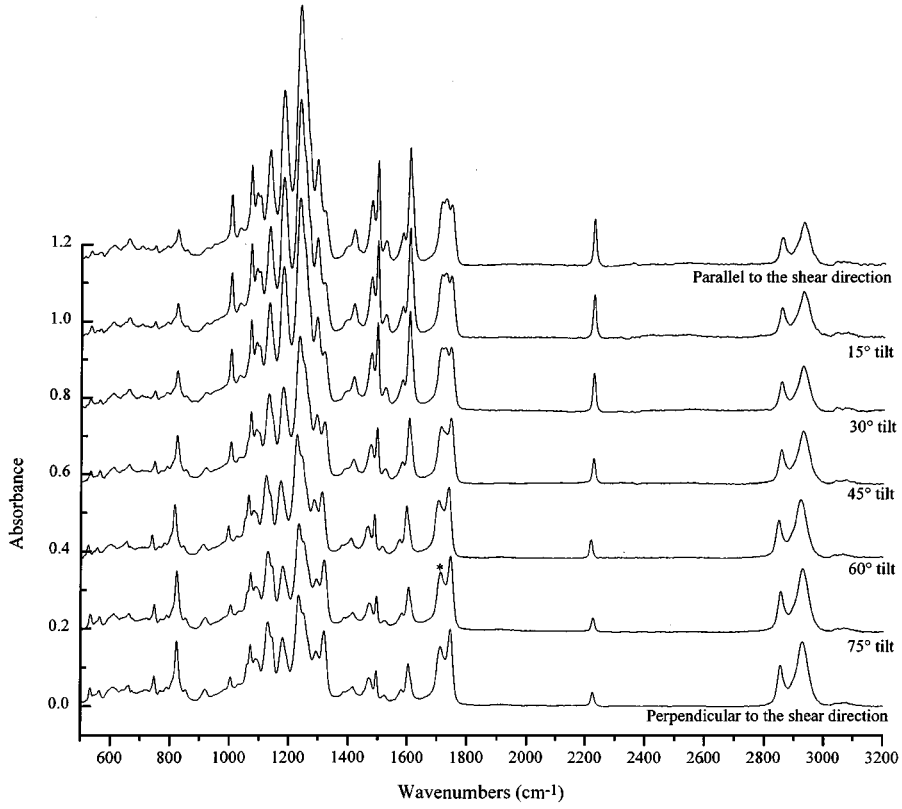

Figure 2 Polarized FT-IR of directly sheared specimens for PEFBP($n = 11$) after rapid quenching to below T_g (recorded at room temperature).

the perpendicular direction than that in the parallel direction, indicating that this stretching is perpendicular to the shear direction. Based on these observations, it can be concluded that both the phenylenes in the backbones and side chains possess an average orientation parallel to the shear direction. This is consistent with our previous structural study on this series of main-chain/side-chain LC polymers in which we found that the low ordered LC nematic (N) phase is constructed by the contribution of both the backbones and side-chain mesogens [21, 23]. They correspond well with published data [31], but possess different intensities due to anisotropic molecular orientations.

In order to study the band topology on different length scales of the sheared PEFBP($n = 11$) films, a tapping mode AFM is employed, utilizing both the height and phase images. A three-dimensional (3-D) topology (height) and corresponding phase image of the band structures in the films can be visualized as shown in Fig. 3a and b, respectively. This film has been quenched from the N phase to below the glass transition temperature, T_g, and therefore, no crystallization occurs. The band structural profile along the shear direction exhibits a sinusoidal trajectory with a spacing of 3 ± 0.5 μm (Fig. 3a). Note that the backbones and side chains are parallel to the shear direction in the N phase based on the polarized FT-IR results and structural analyses [21, 23]. This out-of-plane trajectory is thus sinusoidal along the molecular chain direction. This observation implies that the band structures observed in PLM are due to the alternating change of the optical property (which alternates birefringence), and this is mainly a result of the geometrical difference of the films. When the thickness changes periodically along the shear direction, polarized light beams pass through the samples with different thicknesses to generate optical retardation (which is defined as birefringence times sample thickness). Speculation is that the formation mechanism of the primary bands in the N phase is due to periodic mechanical oscillations during shear. Although the relaxation of chain molecules occurs to affect the chain orientation, the average orientation of the chains seems not to change. Only the orientation distribution becomes broad. This is similar to the AFM observation in contact mode of hydroxypropylcellulose films in air [19].

When the 190 °C-sheared film crystallizes at 105 °C for 12 hours to form the K_{T1} phase [21, 22], the band structure possesses increasing birefringence and sharpened boundaries with crystallization time as observed in PLM (Fig. 4). Within each primary band, apparently fibrillar structures develop in PLM as *secondary bands*. These bands seem to show a zigzag arrangement along the shear direction and within one primary band, the secondary bands tilt around $\pm 30^\circ$ away from the shear direction. The increase in optical birefringence can be deduced to be due to the occurrence of crystallization, which is consistent with the previous study in crystallization kinetics [22]. The spacing of primary bands remains on a scale of 3 ± 0.5 μm. However, the band boundaries are slightly deformed after crystallization. This indicates that the primary bands can only partially confine the crystallization. In fact, crystallization is competing with the constraint of the primary bands at this temperature (above T_g). It is difficult, nevertheless, to directly measure the lateral size of the fibrillar structures in PLM due to the limited resolution.

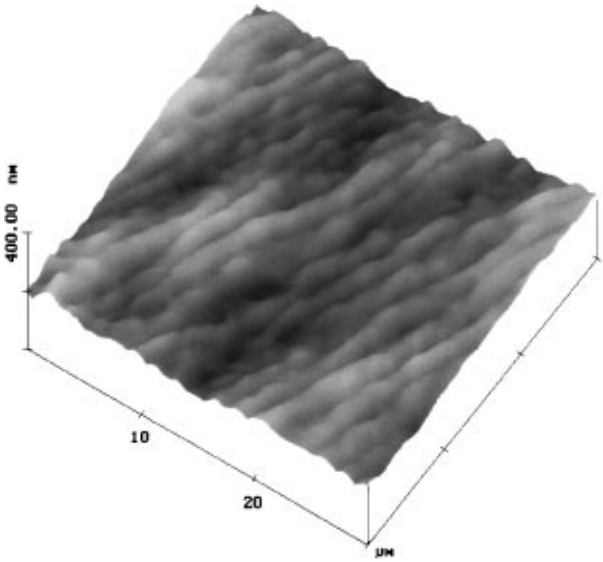

(a)

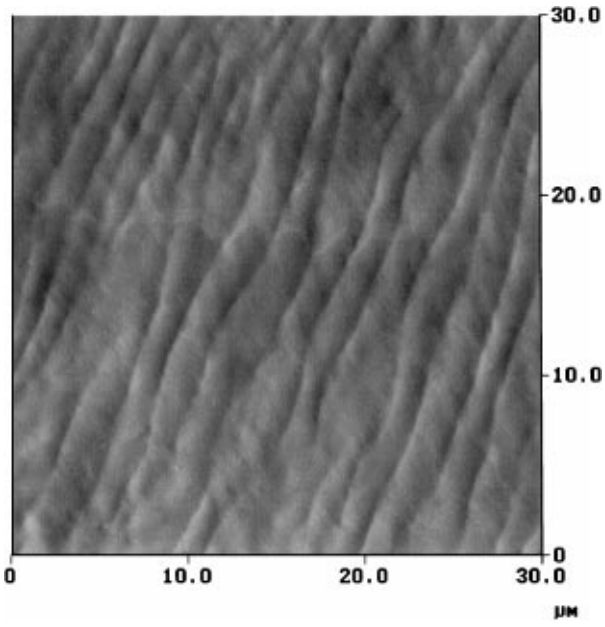

(b)

Figure 3 Tapping mode AFM morphologies of sheared and quenched PEFBP($n = 11$): (a) height image at 30×30 μm^2 scan, (b) the corresponding phase image.

After PEFBP($n = 11$) is isothermally crystallized at 105 °C, polarized FT-IR experiments on the crystallized samples show substantial changes of band intensities as shown in Fig. 5. From this figure, it is evident that changing of the polarized beam orientations from 90° to 0°, the CN groups and the in-plane CH bending of the phenylenes in both the backbones and side chains exhibit monotonic increases. The absolute intensity of the CN vibration at 2225 cm^{-1} decreases substantially at the different rotating angles compared to that before the crystallization. The aliphatic side chains become less anisotropic. The side- and main-chain carbonyl stretching at 1741 and 1722 cm^{-1} shows a maximum at a rotating angle of approximately 0° (as indicated by the * in Fig. 5), indicating that after crystallization of the K_{T1} phase, the carbonyl stretching vibration is parallel to the shear direction. This may imply that the main-chain backbones undergo a possible orientational change. The side-chain carbonyl stretching at 1741 cm^{-1} still shows a maximum intensity parallel to the shear direction, illustrating that this carbonyl stretching is along the shear direction. This observation also supports the conclusion that both backbones and side chains of PEFBP($n = 11$) jointly build up the crystalline K_{T1} phase, as predicted in our structure analyses [21, 23] and molecular motion study [32].

Once the sheared films have been crystallized at 105 °C for 12 hours, a 3-D AFM alternating surface topology of height and phase images is shown in Fig. 6a and b, respectively. In Fig. 6a, the primary bands have a spacing of 3 ± 0.5 μm, and the sinusoidal amplitude variations are 25 ± 5 nm (over 15×15 μm^2). This band structure possesses a similar spacing before crystallization in Fig. 3. From the phase image in Fig. 6b, the secondary fibrillar structures can be seen within the primary bands. A $30 \pm 5°$ tilt angle of the fibrillar direction with respect to the shear direction can be observed. Zigzag structures are observed at a depth ranging from a few to ten nm. This zigzag arrangement of the secondary bands must arise from the occurrence of crystallization partially confined within the shear-induced LC primary bands, which is similar to the case of a random aromatic LC copolyester (mesogenic α-methyl stilbene and flexible spacers with 5 and 7 methylene units in the ratio of 1:1), upon crystallization, observed by transmission electron microscopy after etching [10, 11].

In order to understand the detailed surface and near surface structures within the secondary fibrillar bands, high resolution AFM height and phase images are shown in Fig. 7a and b, respectively (over 1.0×1.0 μm^2). Fig. 7a exhibits 3-D fibrillar bands with a spacing of 250 ± 50 nm and a height variation of 8 ± 2 nm. Interestingly enough, the high resolution AFM phase image in Fig. 7b shows that individual lamellae of approximately 20 nm in thickness are in an edge-on assembled arrangement. These lamellar blocks lead to the fibrillar bands with a 30° tilt angle with respect to the shear direction in each primary band. Consecutive lamellar blocks form zigzag patterns as the secondary bands. These fibrillar bands have also been observed in other main-chain LC polymers after mechanical shearing [33].

An interesting question is why the secondary bands form the zigzag arrangement during crystallization. We speculate that during crystallization, the chain molecules may undergo a self-elongation process. This microscopic length increase along the chain direction may lead to a macroscopic buckling to generate the zigzag arrangement of the lamellar blocks. In order to prove this hypothesis, Fig. 8a shows a WAXD pattern obtained from the oriented films, which are quickly quenched to below T_g after mechanical shearing. In this figure, weak layer reflections can be seen on the meridian, and one pair of halos appear on the equator. This indicates that the quenched phase is the N phase and mesogens in side chains are arranged parallel to the backbones in the shear direction. The layer spacing is 1.94 nm from the (001) reflection on the meridian. The (002) and (004) reflections on the second and fourth layers are also found to be 0.970 nm and 0.485 nm,

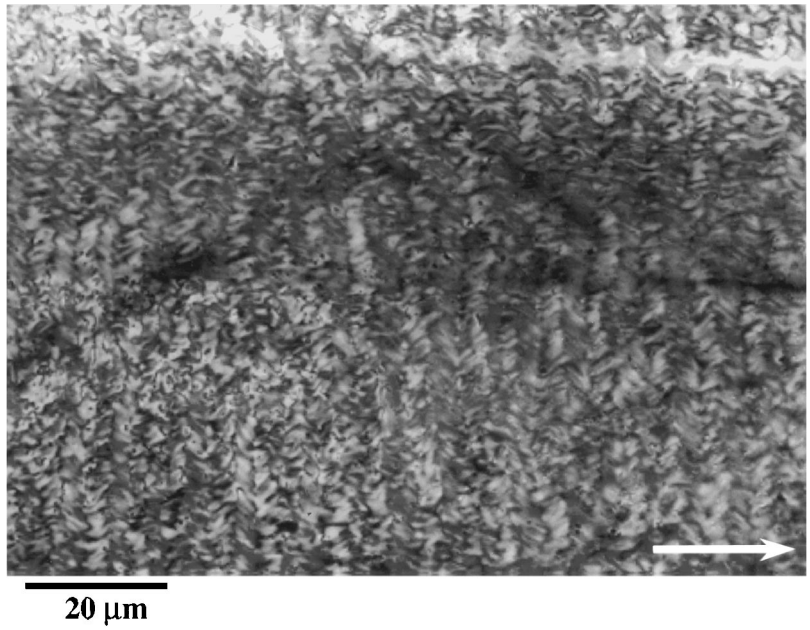

Figure 4 PLM micrographs of directly sheared films for PEFBP($n = 11$) recorded after crystallization at 105 °C for 12 hours (the shear direction is indicated by the arrow).

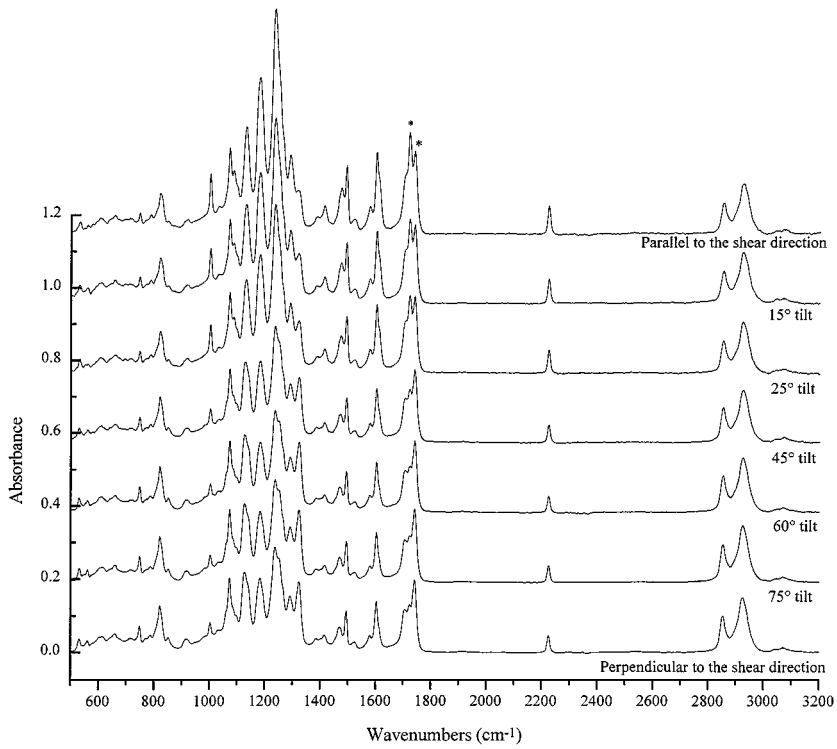

Figure 5 Polarized FT-IR of directly sheared films for PEFBP($n = 11$) recorded after crystallization at 105 °C for 12 hours (recorded at room temperature).

respectively. These results are consistent with our previous structural analyses [21, 23].

After the film was isothermally crystallized at 105 °C for 12 hours, Fig. 8b is the WAXD pattern of the oriented films which exhibit a 3-D crystal (K_{T1}) structure. This leads to a four-chain triclinic lattice based on our structural analyses. The unit cell has dimensions of $a = 1.93$ nm, $b = 1.73$ nm, $c = 2.08$ nm and $\alpha = 90°$, $\beta = 80°$, $\gamma = 93°$ [21]. The *c*-axis dimension represents the extended chain conformation of backbone chemical repeating units. In this crystal structure, the *c*-axis is tilted 38° with respect to the plane normal of flat-on lamellar crystals (the [00l] zone axis), which has been proven by electron diffraction experiments [21]. This K_{T1} crystal formation from the oriented N phase can be viewed as a self-molecular orientational-induced ("soft") epitaxy. This is slightly different from the common study of orientational epitaxy in which one polymer crystallizes on the top of oriented polymer chains [34–36].

The most important observation here is the lattice expansion along the chain direction. An almost 0.14 nm

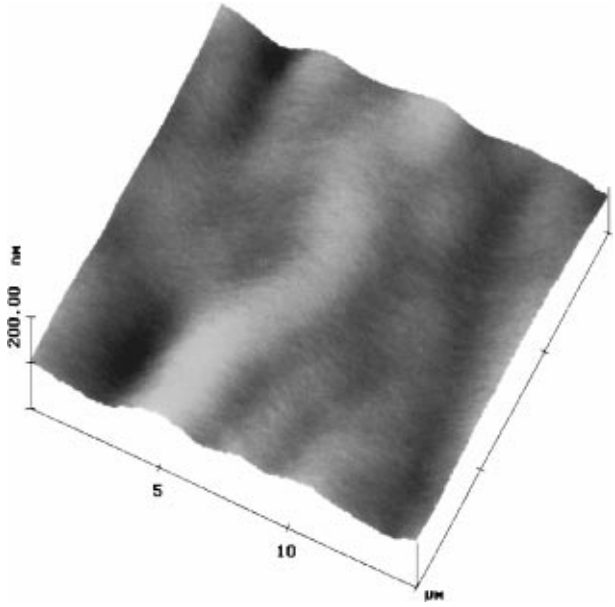

(a)

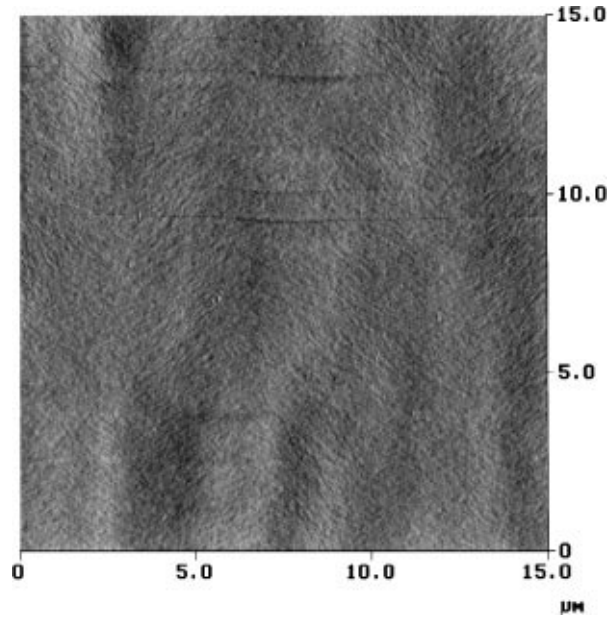

(b)

Figure 6 Tapping mode AFM morphologies of PEFBP($n = 11$) after crystallization at 105 °C for 12 hours: (a) a height image at $15 \times 15\ \mu m^2$ scan, (b) the corresponding phase image.

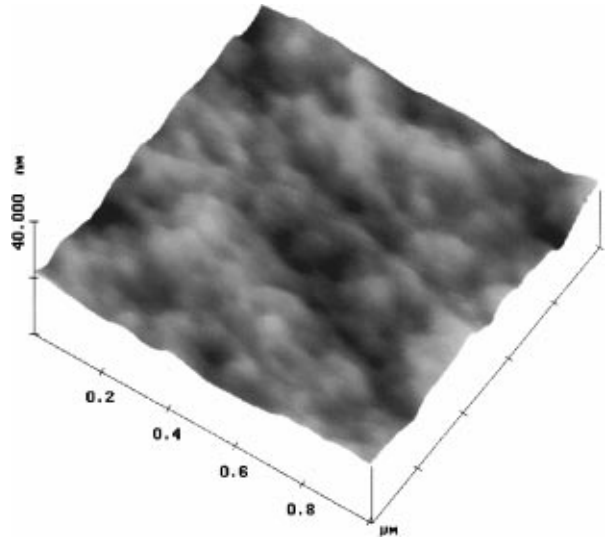

(a)

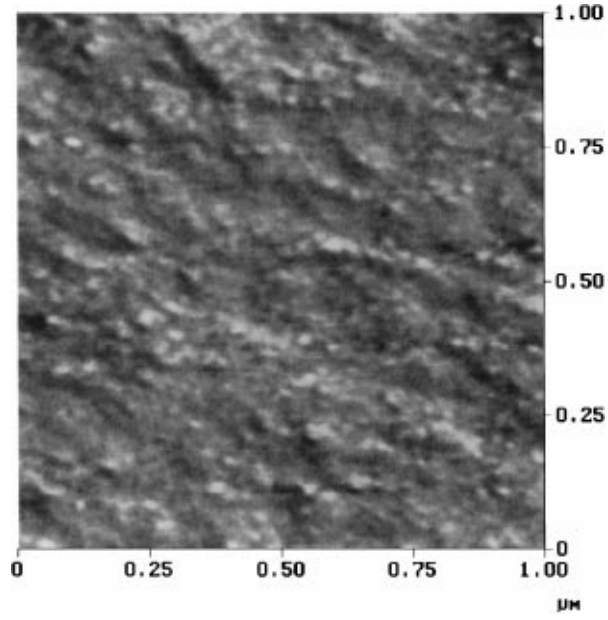

(b)

Figure 7 Tapping mode AFM morphologies of PEFBP($n = 11$) after crystallization at 105 °C for 12 hours: (a) a height image at $1.0 \times 1.0\ \mu m^2$ scan, (b) the corresponding phase image.

expansion after crystallization from the N phase takes place, accompanied by closer lateral packing in the crystals. This accounts for approximately 7% of the length change, which certainly cannot be dissipated, on the microscopic scale without any macroscopic morphological changes. When the lattice expansion occurs in the in-plane direction, the tilt of the *c*-axis is calculated to be 21° with respect to the shear direction after the crystallization. This structural analysis provides direct evidence for the physical origin of macroscopic self-elongation, which further causes the macroscopic buckling to form the ±30° zigzag arrangement of the secondary bands within each primary band.

A schematic representation of different levels of band structures is described based on the shear-induced bands and crystallization-induced bands as shown in Fig. 9. The original LC primary bands are created after the mechanical shear, with a sinusoidal trajectory with a spacing of $3 \pm 0.5\ \mu m$ along the shear direction (Fig. 9a). Upon crystallization, the primary bands remain, but within each band, secondary fibrillar bands of 250 ± 50 nm are formed which consist of lamellar aggregates (Fig. 9b). The individual edge-on lamella possesses a thickness of around 20 nm with the tilted *c*-axis. During crystallization, the microscopic lattice expansion of the dimension along the chain direction leads to a macroscopic in-plane buckling which causes chain tilting and forms the zigzag arrangement of the secondary bands. A molecular model of the chains in each edge-on lamella is also shown in Fig. 9c. Since the *c*-axis of the K_{T1} crystal is always tilted 38° with respect to the plane normal (*n*) of flat-on lamellae [21], and the *c*-axis is tilted 21° with respect to the shear direction due to the lattice expansion, we can calculate that the edge-on lamellar crystals should tilt 31° with respect to

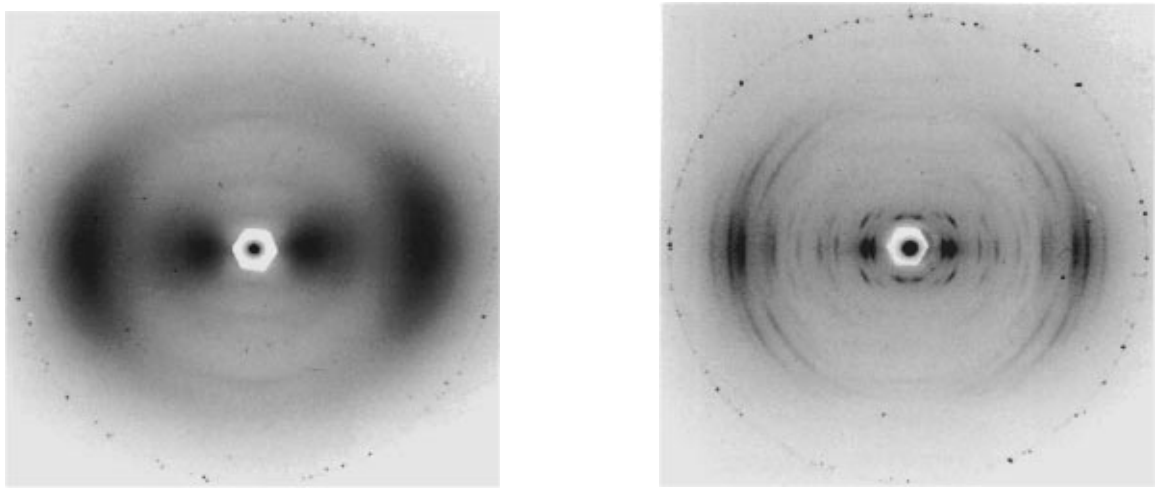

(a) (b)

Figure 8 Wide angle X-ray diffraction patterns of PEFBP($n = 11$) for directly sheared films (a) after rapid quenching to below T_g (recorded at room temperature); (b) after crystallization at 105 °C for 12 hours.

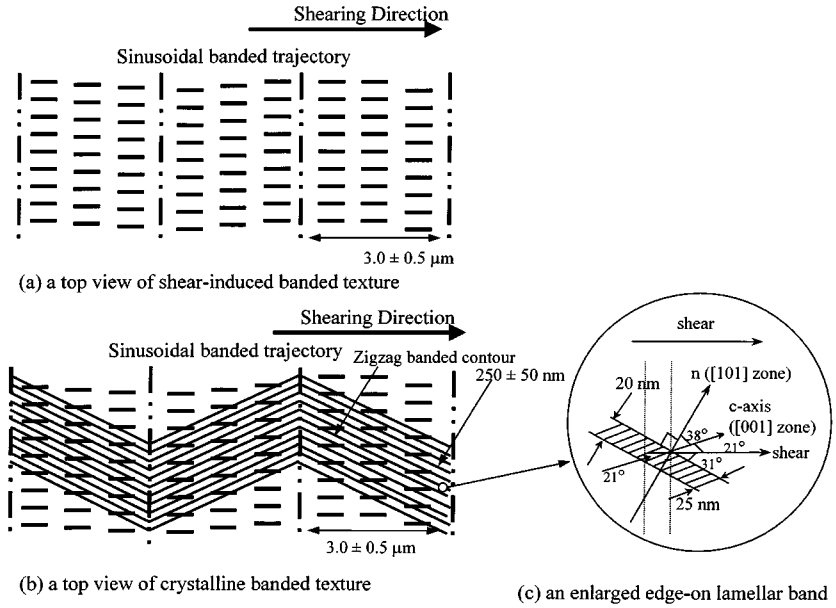

Figure 9 A schematic representative mechanism of band structural formation for PEFBP($n = 11$) from the N phase to the K_{T1} crystalline phase: (a) a top view of shear-induced band structure (primary bands); (b) a top view of the secondary zigzag crystalline bands formed within the primary LC bands; and (c) the origin of constructing an enlarged edge-on lamellar band.

the shear direction. This result is consistent with our experimental observations. The zigzag arrangement also reflects the local minimum of free energy of the molecular packing, which is under a partial confinement of the primary LC bands. A macroscopic chain tilting across many primary bands without the zigzag arrangement needs large molecular cooperative motion and chain reorientation and relocation, of which the free energy is thus not favorable.

4. Conclusion

New elements of band formation have been explored which result from a crystallization process which generates pronounced secondary zigzag bands within the primary LC bands after mechanical shearing as observed by both PLM and AFM. These secondary bands consist of edge-on lamellar aggregates formed during crystallization. Structural evidence provided by WAXD experiments shows that the occurrence of microscopic lattice expansion along the chain direction during the phase transition from the N to the K_{T1} crystalline phase is the physical origin of the macroscopic self-elongation, which causes the buckling that forms the zigzag arrangement. The chain tilting after crystallization has also been proven using polarized FT-IR experiments as comparing the chain orientation in both the N and the K_{T1} phases. A possible packing model on different length scales has been proposed.

Acknowledgements

This work was supported by the National Science Foundation (DMR-96-17030) and the Science and Technology Center for Advanced Liquid Crystal Optical Materials (ALCOM) at Kent State University, Case Western Reserve University and The University of

Akron. During Professor Andrew Keller's visit in December 1998, he was very much interested in these experimental results and enthusiastically discussed them with us, and also encouraged us to further investigate the banding mechanisms. We dedicate this paper to the memory of Professor Andrew Keller and hope that it can serve as a small memorial to his great contributions to polymer science and our lives.

References

1. K. KERKAM, C. VINEY, D. L. KAPLAN and S. J. LOMBADRDI, *Nature* **349** (1991) 596.
2. M. G. DOBB, D. J. JOHNSON and B. P. SAVILLE, *J. Polym. Sci. Phys.* **15** (1977) 2201.
3. G. KISS and R. S. PORTER, *Mol. Cryst. Liq. Cryst.* **60** (1980) 267.
4. T. TAKEBE, T. HASHIMOTO, B. ERNST, P. NAVARD and R. S. STEIN, *J. Chem. Phys.* **92** (1990) 1386.
5. B. E. ERNEST and P. NAVARD, *Macromolecules* **22** (1989) 1419.
6. S. C. SIMMENS and J. W. S. HEARLE, *J. Polym. Sci. Phys.* **18** (1980) 871.
7. C. VINEY, A. M. DONALD and A. H. WINDLE, *J. Mater. Sci.* **18** (1983) 1136.
8. *Idem., Polymer* **24** (1983) 155.
9. M. HOFF, A. KELLER, J. A. ODELL and V. PERCEC, *Mol. Cryst. Liq. Cryst* **241** (1994) 221.
10. *Idem., Polymer* **34** (1993) 1800.
11. M. HOFF, A. KELLER and A. H. WINDLE, *J. Non-Newtonian Fluid Mech.* **67** (1996) 241.
12. C. VINEY and W. PUTNAM, *Polymer* **36** (1995) 1731.
13. C. VINEY and A. H. WINDLE, *J. Mater. Sci.* **18** (1983) 1143.
14. C. VINEY, A. M. DONALD and A. H. WINDLE, *Polymer* **26** (1985) 870.
15. S. E. BEDFORD and A. H. WINDLE, *ibid.* **31** (1990) 616.
16. MACROMOL K. SHIMAMURA, *Chem. Rapid. Commun.* **4** (1983) 107.
17. C. VINEY and A. H. WINDLE, *Polymer* **27** (1986) 1325.
18. S. N. MAGONOV and D. H. RENEKER, *Annu. Rev. Mater. Sci.* **27** (1997) 175.
19. H. FISHER, M. MILES and J. A. ODELL, *Macromol. Rapid. Commun.* **15** (1994) 815.
20. S.-Y. WANG, Ph.D. dissertation, Department of Polymer Science, Akron, Ohio 44325-3909, 1995.
21. J. J. GE, A. ZHANG, K. W. MCCREIGHT, R.-M. HO, S.-Y. WANG, X. JIN, F. W. HARRIS and S. Z. D. CHENG, *Macromolecules* **30** (1997) 6498.
22. J. J. GE, A. ZHANG, K. W. MCCREIGHT, S.-Y. WANG, F. W. HARRIS and S. Z. D. CHENG, *ibid.* **31** (1998) 4093.
23. J. J. GE, P. S. HONIGFORT, R.-M. HO, S.-Y. WANG, F. W. HARRIS and S. Z. D. CHENG, *Macromol. Chem. Phys.* **200** (1999) 31.
24. T. SEKI, M. SAKURAGI, Y. KAWANISHI, Y. SUZUKI, T. TAMAKI, R. FUKUDA and K. ICHIMURA, *Langmuir* **9** (1993) 211.
25. C. S. KANG, H. J. WINKLEHAHN, M. SCHULZ, D. NEHER and G. WEGNER, *Chem. Mater.* **6** (1994) 2159.
26. J. J. GE, G. XUE, F. LI, K. W. MCCREIGHT, S.-Y. WANG, F. W. HARRIS, S. Z. D. CHENG, X. ZHUANG, S.-C. HONG and Y. R. SHEN, *Macromol. Rapid Commun.* **19** (1998) 619.
27. O. HERRMANN-SCHONHERR, J. H. WENDORFF, H. RINGSDORF, P. TSCHIRNER, *ibid.* **7** (1986) 791.
28. M. BALLAUFF and G. F. SCHMIDT, *ibid.* **8** (1987) 93.
29. A. ADAM and W. SPIESS, *ibid.* **11** (1990) 249.
30. H. R. KRICHELDORF and A. DOMSCHKE, *Macromolecules* **29** (1996) 1337.
31. G. SCRATES, "Infrared Characteristics Group Frequencies" (John Wiley & Sons: Chichester, UK, 1980).
32. J. J. GE, M. GUO, J. Z. ZHANG, P. S. HONIGFORT, I. K. MANN, S.-Y. WANG, F. W. HARRIS and S. Z. D. CHENG, *Macromolecules* **33** (2000) 3983.
33. Y. YOON, A. ZHANG, R.-M. HO, S. Z. D. CHENG, V. PERCEC and P. CHU, *ibid.* **29** (1996) 294.
34. J. C. WITTMANN and P. SMITH, *Nature* **352** (1990) 414.
35. P. DAMMAN, M. DOSIERE, P. SMITH and J. C. WITTMANN, *J. Am. Chem. Soc.* **117** (1995) 1120.
36. P. DAMMAN, M. DOSIRE, M. BRUNEL and J. C. WITTMANN, *ibid.* **119** (1997) 4333.

Received 8 March
and accepted 10 March 2000